sciendo

DOI: 10.2478/ata-2022-0025

Acta Technologica Agriculturae 4
Nitra, Slovaca Universitas Agriculturae Nitriae, 2022, pp. 169–175

PERFORMANCE EVALUATION OF TILLAGE KNIFE DISCHARGE MICROCHANNEL

Khozhakeldi TANBAYEV[1], Sayakhat NUKESHEV[1]*, Adilet SUGIRBAY[2]

[1]S. Seifullin Kazakh Agro Technical University, Technical Faculty, Nur-Sultan, Kazakhstan, khozhakeldi.tanbayev@kazatu.kz
[2]Northwest A & F University, College of Water Resources and Architectural Engineering, Yangling, Shaanxi Province, China, s.adilet.93@gmail.com

*correspondence: s.nukeshev@kazatu.kz

Liquid mineral fertilizers (LMF) have a high sorption ability, can be metered precisely, and the intra-soil application of LMF is relevant. However, the agricultural equipment for this process that introduces the liquid fertilizer under processed soil layer in the form of a wide band has not yet been proposed. The purpose of the study is to evaluate the performance of a 102 mm wide rectangular discharge microchannel of the proposed soil tillage knife designed for deep tillage and intra-soil application of liquid fertilizers and to study the influence of the microchannel length (*L*) and slot height (*h*) on the uniformity of discharge. Solidworks Flow Simulation® was used during investigations, and simulation results were compared with experiment results. It has been determined that the effective slot height for water discharge at V_i = 3–4 m·s^{-1} is 0.1 (±0.01) mm, an effective microchannel length is 20 (±2) mm, and the influence of *L* depends on *h*. Sheet thickness will not change at a distance of 10–15 mm (*b*). Fall angle is 0–5°. In conclusion, the proposed discharge microchannel with asymmetrical feed is applicable for intra-soil application of LMF, and the surface tension effect has to be considered. A way to enhancing the sheet uniformity is the geometrical modification of feed channel shape.

Keywords: chisel plough; discharge uniformity; flow simulation; mineral fertilizer; slot distributor; soil cultivation

The initial basis of this study is soil fertility problems (Kurishbayev et al., 2020; Nguemezi et al., 2020; Nouraein et al., 2020). The development of a working body for soil cultivation and intra-soil application of liquid mineral fertilizers that is more efficient, environmentally friendly, and applicable for variable-rate application systems (Yamin et al., 2016; Sugirbay et al., 2020) is essential. During the evaluation, the related investigations (Kostikov et al., 2016; Xiuyun et al., 2019; Vasilyev et al., 2020) and design features of current soil-processing tools in operation (sweep paw, knife fertilizers, chisel fertilizers) with mounted spraying elements such as nozzle, pipe, injector, or orifice, have been analysed. Accordingly, innovative novelties of well-known manufacturers, which engaged in the development and manufacturing of mechanisms, working bodies, and components that exploited in LMF application processes, have been studied. Many manufacturers, for example, offer tools with a disk working body, where the LMF delivery nozzle (pipe) is installed behind the disk and moisturizes the furrow without capacious spraying. The liquid controlling and delivering system FurrowJet (Precision Planting, 2018) places the bands of fertilizer on and near the seed (3 lines) in starter fertilizing. The openers with the Triplex Injection system have the narrowest opener design for nutrient application with low soil disturbance (Exactrix® Global Systems LLC, 2013).

A uniform planar subsoil application of LMF gives more effective results (Vasilyev et al., 2020). However, the agricultural equipment for this process that introduces liquid fertilizers in the form of a wide band has not yet been proposed. Relevantly, the design of a tillage knife with an internal rectangular microchannel and cylindrical feed channel with the liquid delivered from one side, has been proposed (Tanbayev, 2022). Accordingly, the question about discharge uniformity efficiency that depends on outlet velocities (V_o) uniformity (*U*) was raised.

The flow in the feed channel that streams to the end of the channel and then passes through the sidelong slit to the rectangular microchannel (Kandlikar and Grande, 2003; Steinke and Kandlikar, 2006; Bourhane and Yassine, 2021) is similar to the flow conditions and discharge characteristics of perforated-pipe distributors (Wang, 2011; Liu et al., 2017; Ibrahim et al., 1986), and much more of slot distributors (Tilton, 2007). Many research results indicated that the continuous single-slot geometry yielded the most uniform outflow and the single-slot-equipped manifold has a clear advantage with the simplicity of manufacture. Chen and Sparrow (2009) investigated the efficacy of three types of exit-port geometries, and one of them – a single, continuous longitudinal slot that coincides with our concept. A few researchers suggested obstacles in the feed channel to obtain the sheet uniformity. Senecal (1957) showed under which certain conditions the flow from a slotted pipe becomes maldistributed and suggested to lengthen the lips that provide an increase in pressure drop across the slot. Consequently, the microchannel length (*L*) with an estimated slot height (*h*) in our design will provide an effect of lips or an obstacle, and increasing the microchannel length gives a positive effect in obtaining the uniform liquid sheet that guarantees the uniform distribution of LMF along the slot. In parallel with discharge uniformity, the ways of evaluation of discharge uniformity were studied as well. Hassan et al. (2014) used a non-uniformity (Φ) equation to evaluate the flow distribution. Tilton (2007) proposed the percent

maldistribution, defined as the percentage variation in the flow between the first and last holes. Overall, investigation has shown that the studies relating slot distributors are limited.

The objectives of this paper are:

1. the performance verification of the proposed rectangular discharge microchannel with a slot opening;
2. investigation of the impact of the microchannel parameters such as h, *L* on the forming liquid sheet and consequently on discharge uniformity;
3. evaluating the visual characteristics of the obtained liquid sheet;
4. defining the possible sheet uniformity criteria.

The idea is the application of a tillage knife with rectangular discharge microchannel and asymmetrical feed channel with advantages in terms of low soil-tool interaction. The novelty of this work is in the design parameters of the discharge microchannel, in the method and criteria of evaluating the discharge uniformity, and in suggestions for improving the sheet uniformity.

Material and methods

Description of the 3D model for computational simulations and set of parameters

The computational simulations were performed using the Solidworks Flow Simulation®. Water was used as the fluid medium, the surface tension σ_s = 0.0728 N·m^{-1}, ρ = 997.56 kg·m^{-3}, and these conditions have been considered in laboratory experiments (T = 20–25 °C). Internal analyses were applied to simulations, the inlet velocities range was V_i = 1–6 m·s^{-1}.

The number of 3D models of the knife working part (Tanbayev, 2022) with the slot height h_1 = 0.1 mm, h_i = 0.12319 mm, h_2 = 0.15 mm, h_3 = 0.2 mm, h_4 = 0.25 mm, h_5 = 0.3 mm, and with the L values ranging between 1 mm and 30 mm, has been created. The outer length of the model is 105 mm, the height is 4.8 mm. The feed channel diameter (d = 4 mm) and slot width (w = 102 mm) is constant (Fig. 1). The second end of the feed channel is conditionally plugged with a lid. The cross-section area of the cylindrical feed channel or inlet area (A_i) is 12.56 mm^2. If the outlet area is $A_o = h_w$, and $A_i = A_o$, correspondingly, h will be equal to 0.12319 mm. It is the initial height (h_i) that provides the conveyance capacity of the microchannel, and the $h > h_i$ and $h_i < h$ conditions will also be investigated.

To obtain the data, two types of engineering goals (set of parameters) were used: the point and the surface goals. In the rectangular microchannel, two lines of point goals were applied: the Microchannel End Line (MEL) – at the outlet and the Microchannel Initial Line (MIL) – at the transition line. In the cylindrical feed channel, the lines of point goals were applied (CAL). The interval of parametrical points (Z_p) on each line is 1 mm, and so there are 102 (n) parametrical points on the MEL and MIL, and 106 parametrical points on the CAL.

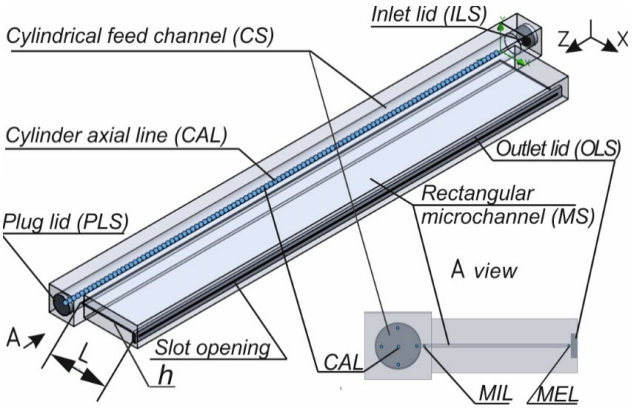


Fig. 1 Conditional 3D model of tillage knife and designated engineering goals

The following boundary conditions were determined: inlet velocity (3 m·s^{-1}) – on the inlet lid, environment pressure (P = 101,325 Pa) – on the outlet lid, and real wall – on the plug lid, on the Surfaces of Microchannel and Cylindrical feed channel (Fig. 1). The following surface goals were determined: Inlet Lid Surface (ILS), Cylinder Surface (CS), Plug Lid Surface (PLS), Microchannel Surface (MS), and Outlet Lid Surface (OLS).

More than 150 simulation runs were performed. Obtained visual results were compared with experimental results (videos, photo). The generated velocity indicators at each Z_p were saved in Excel files, and comparative tables and graphs were created. The dependencies were analysed using TIBCO Statistica®. About 4300 cases of V_o (m·s^{-1}) were entered into the statistical spreadsheet for analyses.

Analyses show that the flow uniformity index at Solidworks Flow Simulation® and ordinary coefficient of variations (C_v) could not assess the uniformity. To determine the dimensionless index (U), which evaluates the uniformity of the resulting sheet, Eq. 1 has been proposed.

$$U = \left(50 \left(\frac{V_{min1}}{V_{max3}} + \frac{V_{min3}}{V_{max1}} \right) \cdot \frac{V_{min2}}{V_{max2}} \right) \cdot \frac{V_{m1} V_{m3}}{V_{m2} V_i} \cdot r \quad (1)$$

where: r – equal to A_i/A_o when $A_i < A_o$ and equal to A_o/A_i when $A_i > A_o$

Accordingly, the outlet velocity indicators (or all point parameters line) at all analyses, at all cases of simulation were conditionally divided into three parts. The V_{max}, V_{min} values of outlet velocities, and outlet mean velocity V_m were defined for each part. The mentioned parameters give the overall uniformity of data and provide evaluation of the sheet symmetry. Moreover, the V_i impact was also taken into account, and it shows the power of expected V_o. Equation 1 is acceptable only for liner (point) parameters of simulation results.

Description of experimental set-up

Figure 2 shows the scheme of the experimental installation with 10 discharge (outlet) pipes and a tillage knife sample (photo) made of plexiglasses. One pipe is selected to feed the experimental knife sample (1), and the others flow back to the tank without any obstacles. The outer dimensions

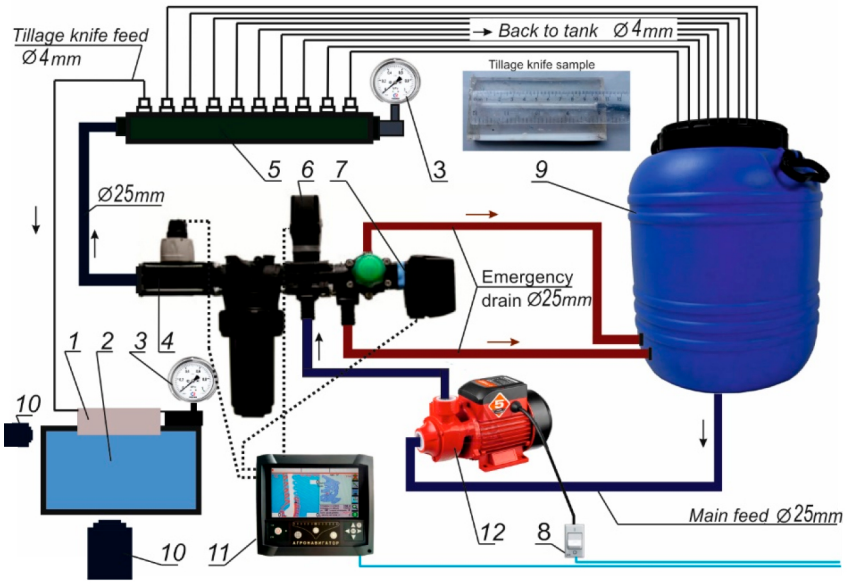


Fig. 2 Scheme of the experimental installation and tillage knife
1 – experimental knife sample; 2 – water collection vessel (30 L); 3 – pressure gauge (0.6 MPa); 4 – flowmeter; 5 – distributor; 6 – electric main control valve; 7 – electric proportional control valve; 8 – switch; 9 – tank (50 L); 10 – video cameras; 11 – onboard computer; 12 – surface pump (400 kW, 35 L·min^{-1})

of the experimental samples (1) are 110 × 52 × 10 mm and they are made in many variants with different values of *L* and *h*.

During the experiments, the following features were visually evaluated: the fullness of the sheet regarding slot width ($w = w_1$), sheet shape, sheet symmetry or perpendicularity, fall angle (α), rim angle (γ), and flow characteristics in the cylindrical feed channel and microchannel. The uniformity of the liquid amount that flowed out along the slot of microchannel was measured with a handmade plastic multicellular measuring tube (Fig. 7f) at the instant time (0.4–0.5 s).

The liquid amounts in each cell (tube) were defined, and the coefficient of variation of indicators was calculated. Then, C_v and U were compared.

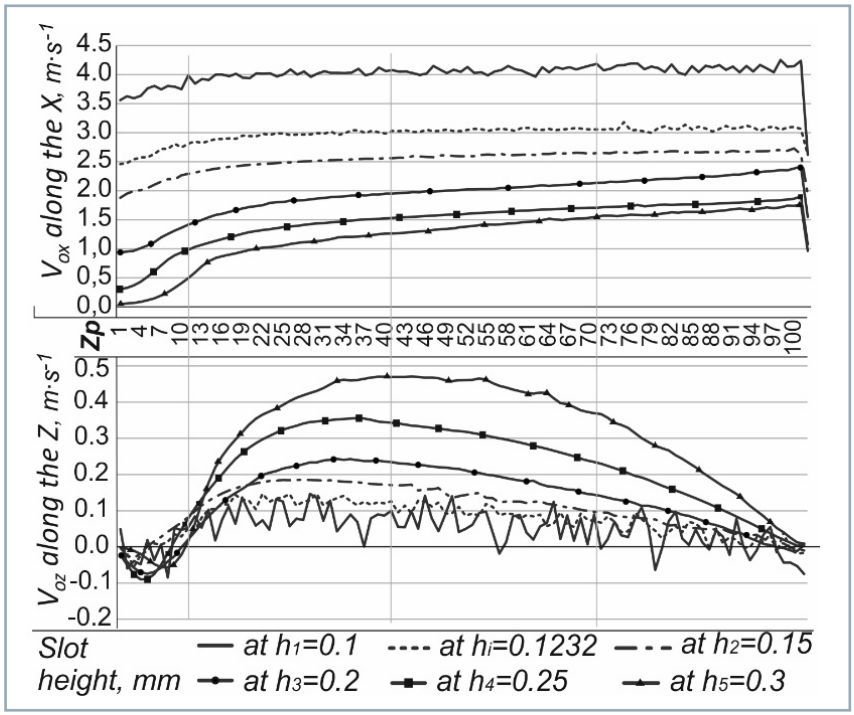


Fig. 3 Graphs of the outlet velocity along the *X*-axis (V_{ox}) and *Z*-axis (V_{oz}) at different slot height
Z_p – specified points along the *Z*-axis

Results and discussion

Slot height impact

The calculated Reynolds number range in rectangular microchannel was 50–2,400, here $D_h = 2\,h$ as the w/h ratio is excessively high. Experimental and visual (simulation) results also show that laminar flow is formed in the microchannel. When the slot height is h_3, the displacement of flow, lower outlet velocity, and emptiness at the initial part of the microchannel are noticed. When the slot height is h_5, displacement and emptiness have raised. Similar phenomena have been observed during the experiments.

The total pressure is high, i.e. 0.18 MPa at h_1 (L = 0.15 mm) and 0.15 MPa at h_i, and low, i.e. 0.11 MPa at h_3. Accordingly, the pressure drop is high at h_1 and h_i, so it provides a sufficient discharge uniformity.

Figure 3 presents the graphs of V_{ox} and V_{oz} related to models with L = 14 mm and with different values of slot height (h). It can be seen that at h_1 the outlet velocity along the *X*-axis is higher (about 4 m·s^{-1}), and correspondingly the velocity along the *Z*-axis is very low (0.1 m·s^{-1}). At h_i, velocity (V_{ox}) approaches the inlet velocity (3 m·s^{-1}), and V_{oz} reaches 0.19 m·s^{-1}. At h_3, velocity (V_{ox}) decreases as stated above, and V_{oz} reaches 0.25 m·s^{-1}, which means that displacement of flow (or liquid particles) emerges. When h_5 = 0.3 mm, V_{oz} reaches up to 0.5 m·s^{-1}.

The analysis shows that the slot height directly affects the discharge uniformity as well as the sheet formation. It can be concluded that by decreasing the slot height, the displacement of particles is reduced, outlet velocity is increased, and the graph of outlet velocity becomes more stable. If the slot height is high inaccurately to inlet velocity, the liquid simply flows out in the middle of the slot symmetrically, in an equilateral triangle form, and with a weak outlet velocity, as well as without filling

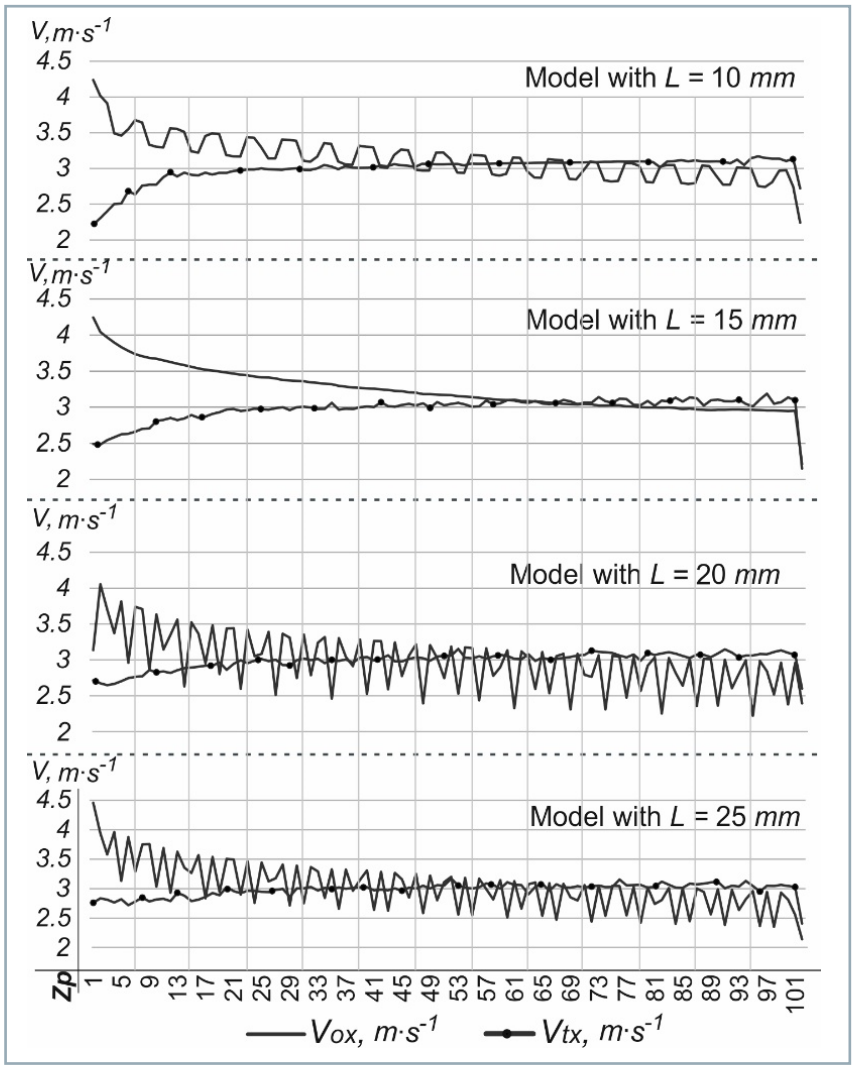


Fig. 4 Comparison of V_{ox} and V_{tx} velocities at different L
Z_p – specified points along the Z-axis

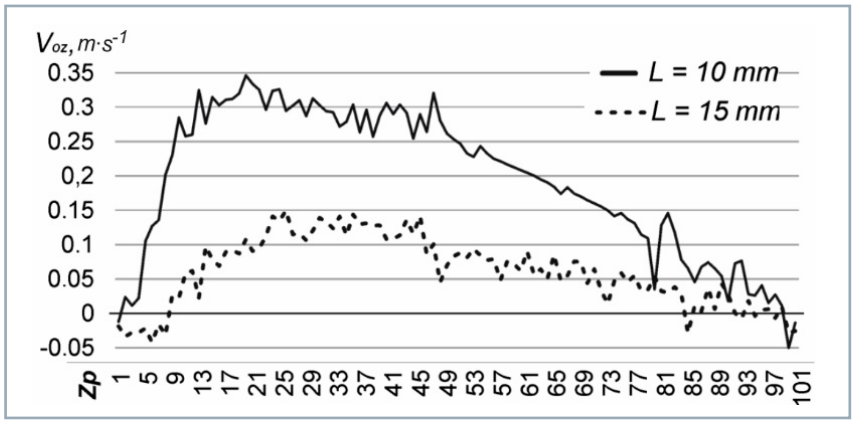


Fig. 5 Comparison of V_{oz} velocities at different L
Z_p – specified points along the Z-axis

the slot width ($w_1 < w$). In contrast, if inlet velocity is higher inaccurately to the slot height, the spray sheet moves away from the feed side, and the liquid flows out with pressure forming an acute triangle ($w_1 < w$). It is important to find the appropriate slot height at desired feed velocity considering the LMF application doses. In economic point of view, 3 m·s^{-1} is the upper limit.

At h_1, A_i/A_o = 1.23, however, the V_{oxavg}/V_i ratio ranged from 1.34 to 1.23. Equality has occurred with large values of L (28–30 mm). At h_2, A_i/A_o = 0.82, however, on many models of L, the V_{oxavg}/V_i ratio was 0.84. Equality was observed with low values of L (5–10 mm). The average correction factor for calculating the V_{oavg} according to given V_i is 1.06 at h_1, 1.08 at h_2, and 1.02 at h_3.

According to simulations, the models with the slot height h = 0.1 (±0.01) mm have shown effective results in terms of sheet uniformity at the 3–4 m·s^{-1} feed velocity.

Microchannel length effect on sheet uniformity

Figure 4 demonstrates the velocity graphs of models with h_i and L = 10 mm, L = 15 mm, L = 20 mm, and L = 25 mm. It compares the outlet velocities along the X-axis obtained from MEL for each model and similarly, velocities at the transitional line obtained from MIL. It is noticeable that when the L value is low (L = 10 mm), the initial part of V_{ox} is lower. Additionally, the start value of V_{ox} is very low (2.2 m·s^{-1}), and the graph just after 10–12 specified points (Z_p) stabilizes. When the L value is high (L = 25 mm), the graph of V_{ox} is stable almost for the whole slot, and the start value of V_{ox} is 2.7 m·s^{-1}. The graph of V_{tx} has a similar decreasing trend in all models.

The graph becomes more stable by increasing L because the displacement of liquid particles along the Z-axis diminishes (Fig. 5). However, in some cases, V_{oz} has a negative value at the initial specified points, and it can negatively affect the uniformity. A uniform transition of flow at the transition line (MIL) is essential and it can be provided by uniform pressure distributions in the cylindrical feed channel.

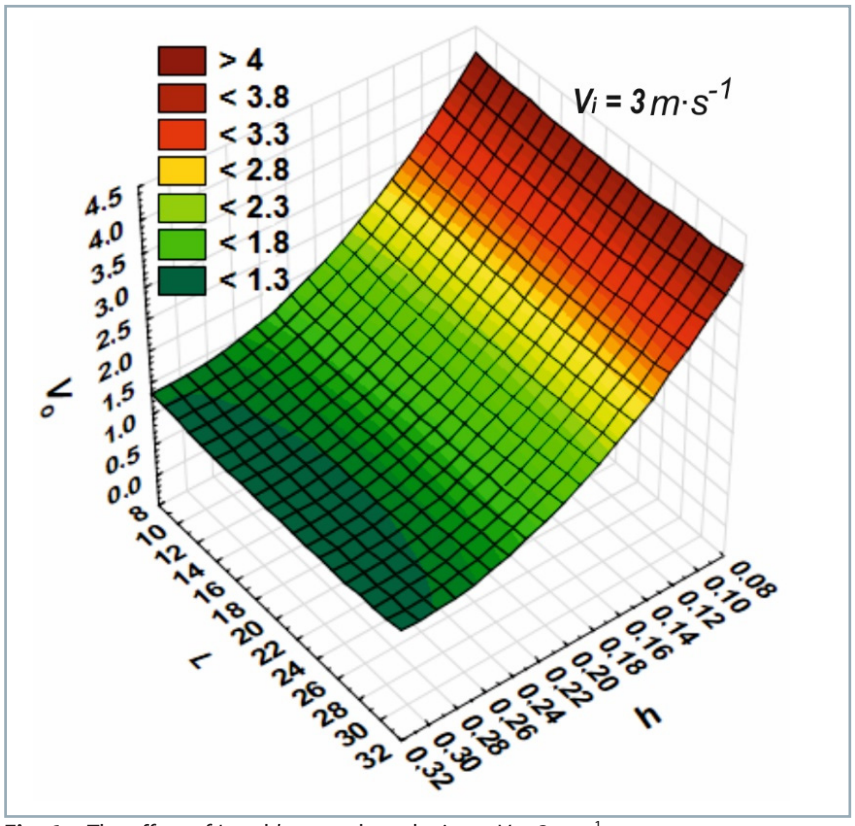


Fig. 6 The effect of L and h on outlet velocity at V_i = 3 m·s^{-1}

By prolonging the microchannel length, the volume of the rectangular microchannel increases and it leads to rising the internal resistance. As a result, total pressure rises. For example, in the model with h_1 = 0.1 mm and L = 6 mm, total pressure is 0.16 MPa, by contrast to the model with L = 30 mm, where it reaches 0.29 MPa in the feed channel. An increase in the internal pressure mainly in the cylindrical feed channel ensures the outlet velocity uniformity, as a result of the sheet shape.

Overall, the statistical analyses show that the parameters L, h, and V_i are closely interconnected and have a multidirectional effect on uniformity. Indeed, the impact of h is more significant than the impact of L and is polynomial (Fig. 6). The effect of L needs to be evaluated only with effective values of h, and the microchannel elongation has a positive effect only at certain values of L, then it becomes constant or has a negative effect. A way to enhancing the sheet uniformity is the geometrical modification of feed channel shape.

Experimental confirmation of computational results

A uniform water sheet was obtained only at 2.78 m·s^{-1} and higher inlet velocities. When the liquid is sprayed with a low velocity, or if h is high, surface tension induces a force that contracts the shape of the liquid into a thick rim (Carvalho et al., 2002). The liquid simply vanishes without filling the slot at low inlet velocity. Bubble and annular flow modes were observed only at high values of h and V_i. It is noted that sheet thickness will not change at the 10–15 mm length (b) and fall angle (α) 0–5°. The b, α and rim angle (γ) is needed to predict the colliding width (w_0).

Figure 7 compares the sheet uniformity sprayed from the knife samples with different L and h values. The water sheet from the sample with h_2 and L = 30 mm is more stable than others and is perpendicular (Fig. 7a), U = 74%. It has a full triangle liquid sheet. Unfortunately, the formed liquid sheet is not fully symmetrical, and the left-hand rim goes under the right-hand rim (it was notable in models with high L). That is because the outlet velocity in the end part of the slot is lower than the outlet velocity in the initial side. Additionally, Fig. 7a contains given dimensions of obtained effective trapezoid according to conditionally chosen b = 13.2 mm. However, the expected colliding width is undesirably low, w_0 = 78.1 mm.

By increasing the slot height, uniformity was disrupted. Although the water sheet from the sample with h_3 and L = 30 mm is symmetrical (Fig. 7b), it slowly moves away from the feed side (U = 48%) and the rim becomes

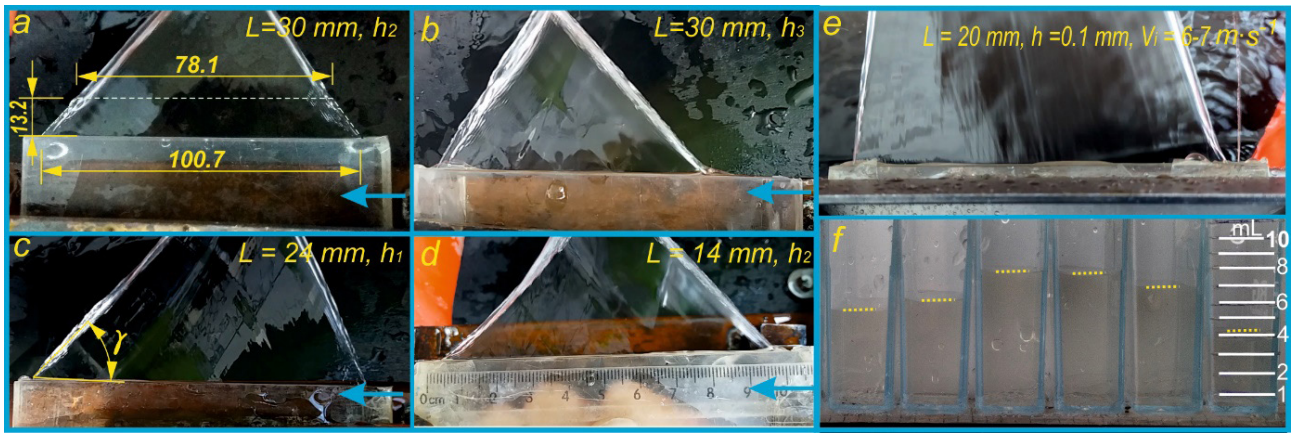


Fig. 7 Liquid sheets obtained from experimental samples

large (here $w_1 < w$). A similar situation was reported also by Olson (1981). They have linked this process with the ratio (A_o/A_i), the pressure recovery would be large near the closed end if the ratio becomes much greater than required. Indeed, the ratio depends on the slot height. In the knife sample with h_1 and L = 24 mm, symmetry violation (feed side rim angle less than another side rim angle) is connected with low inlet velocity, and low velocity particularly at the final part of the slot, U = 84% (Fig. 7c). It can be seen that in the sample with L = 14 mm, h_2 has a sufficient sheet with an arc-shaped rim, U = 54%. It means that slot height is higher than required and L is lower, thus creating a weak outlet velocity in the microchannel slot (Fig. 7d). Even in models with h_2 and L = 30 mm and with h_1 and L = 24 mm, C_v was below 60% and the main reason for this is the surface tension phenomenon.

Surface tension can be surpassed by increasing the inlet velocity. Figure 7e presents the liquid sheet in trapezoidal shape obtained at the 6 m·s^{-1} inlet velocity, U = 88%. The coefficient of variation of the liquid amount filled in the measuring tube (Fig. 7f) is C_v = 78%. The deviation between C_v and U is 11%. Unfortunately, high velocity leads to high consumption of LMF, which is economically unacceptable. Overall, the deviation between C_v and U was in the range of 5–15%. It is assumed that deviations are due to surface tension and mechanical defects (low percentage) in manufacturing processes. Surface tension is unaccounted for in the simulation runs.

Since the LMF application process takes place under a deep soil layer, the surface tension phenomenon will not have an effect because the LMF flow collides with soil particles at the same time as the air. Therefore, in such cases a low feed rate (2–4 m·s^{-1}) can be effective. However, it must be verified by field experiments.

In terms of mechanical aspect, an unnecessary low slot height and a large microchannel length increase the workload of the pump or the whole system. Experimental results confirmed the effectiveness of the slot height h = 0.1 (±0.01) mm and the microchannel length L = 20 (±2) mm.

Conclusion

In conclusion, the proposed discharge microchannel is applicable for obtaining the uniform liquid sheet with the required width and outlet velocity. Uniform outlet velocity not only indicates discharge uniformity but also it is important for evaluating the impact force of the sheet. Slot height (h) and length (L) are essential for obtaining the uniform sheet when exploiting liquids with different viscosity.

Slot height directly affects the sheet forming and uniformity. By increasing of h, outlet velocity decreases, and by decreasing of h, the displacement of particles is reduced and pressure in the feed channel increases. Consequently, pressure drop rises, and, as a result, V_o uniformity becomes more stable. The increasing of the L value provides an increase in internal pressure mainly in the cylindrical feed channel and affects the liquid sheet and discharge uniformity. In its turn, it slightly depends on the slot height.

The values of h = 0.1 (±0.01) mm and L = 20 (±2) mm are the effective parameters for obtaining the uniform sheet when using the water and at V_i = 3–6 m·s^{-1}. Sheet thickness will not change at a distance of 10–15 mm.

A water sheet with α = 2–3°, $\gamma \approx$ 80–85°, and C_v = 70–80% at the inlet velocity V_i = 6 m·s^{-1} was experimentally obtained using the model with h = 0.1 mm and L = 20 mm. The calculated indicators of uniformity were U = 85–90%. The deviation between C_v and U was 11%. Overall, the deviation between C_v and U was in the range of 5–15%, and the influence of surface tension phenomenon has been observed. Surface tension can be surpassed by increasing the inlet velocity, however, the LMF distribution dose must be considered. Uniformity can be enhanced by geometrically modifying the feed channel.

References

BOURHANE, B. – YASSINE, K. 2021. Numerical study of laminar forced convection of nanofluid in a new microchannel heat sink. In Strojnícky časopis – Journal of Mechanical Engineering, vol. 71, no. 2, pp. 31–40.

CARVALHO, I. – HEITOR, M. – SANTOS, D. 2002. Liquid film disintegration regimes and proposed correlations. In International Journal of Multiphase Flow, vol. 28, no. 5, pp. 773–789.

CHEN, A.W. – SPARROW, E. 2009. Effect of exit-port geometry on the performance of a flow distribution manifold. In Applied Thermal Engineering, vol. 29, no. 13, pp. 2689–2692.

EXACTRIX® GLOBAL SYSTEMS LLC. 2013. P-51 Mustang. Available at: http://www.exactrix.com/mustang.htm

HASSAN, J. M. – MOHAMMED, W. S. – MOHAMED, T. A. – ALAWEE, W. H. 2014. CFD simulation for manifold with tapered longitudinal section. In International Journal of Emerging Technology and Advanced Engineering, vol. 4, no. 2, pp. 28–35.

IBRAHIM, T. – RAYMOND, A. – BRYANT, A. 1986. An investigation of flow distributions in perforated pipes. In Proceedings of the 9th Australian Fluid Mechanics Conference. Auckland : Australia, pp. 292–296.

OLSON, D. A. 1981. Water Flows Slotted from Pipes. Solar Energy Research Institute. A Division of Midwest Research Institute. Report No.: TR-631-984/UC-64. Contract No. EG-77-C-0.1-4042.

KOSTIKOV, I. F. – BOGALOV, I. M. – TANBAYEV, K. 2016. The device for creating of mineralized strip of fire-prevention purpose. In Science News of Kazakhstan, vol. 3, no. 129, pp. 111–119. (In Russian: Ustroistvo dlya sozdaniya mineralizovannoi polosy protivopozharnogo naznacheniya)

KURISHBAYEV, A. K. – CHERNENOK, V. G. – NURMANOV, Y. T. – PERSIKOVA, T. F. – ZHANZAKOV, B. Z. – KUZDANOVA, R. S. – SERIKPAEVA, Z. K. 2020. Meaningful management of soil fertility and flax productivity. In Arabian Journal of Geosciences, no. 13, article no. 787.

LIU, H. – ZONG, Q. – LV, H. – JIN, J. 2017. Analytical equation for outflow along the flow in a perforated fluid distribution pipe. In Plos One, vol. 12, no. 10, article no. e0185842.

NGUEMEZI, C. – TEMATIO, P. – YEMEFACK, M. – TSOZUE, D. – SILATSA, T. 2020. Soil quality and soil fertility status in major soil groups at the Tombel area, South-West Cameroon. In Heliyon, vol. 6, no. 2, article no: e03432.

NOURAEIN, M. – KOUCHAK-KHANI, H. – JANMOHAMMADI, M. – MOHAMADZADEH, M. – ION, V. 2020. The effects of tillage and fertilizers on growth characteristics of Kabuli chickpea under Mediterranean conditions. In Acta Technologica Agriculturae, vol. 23, no. 1, pp. 18–23.

PRECISION PLANTING. 2018. FurrowJet. Available at: https://www.precisionplanting.com/products/product/furrowjet

KANDLIKAR, S. G. – GRANDE, W. J. 2003. Evolution of microchannel flow passages –thermohydraulic performance and fabrication technology. In Heat Transfer Engineering, vol. 24, no. 1, pp. 3–17.

SENECAL, V. E. 1957. Fluid distribution in process equipment. In Industrial & Engineering Chemistry, vol. 49, no. 6, pp. 993–997.

STEINKE, M. E. – KANDLIKAR, S. G. 2006. Single-phase liquid friction factors in microchannels. In International Journal of Thermal Sciences, vol. 45, no. 11, pp. 1073–1083.

SUGIRBAY, A. M. – ZHAO, J. – NUKESHEV, S. O. – CHEN, J. 2020. Determination of pin-roller parameters and evaluation of the uniformity of granular fertilizer application metering devices in precision farming. In Computers and Electronics in Agriculture, vol. 179, article no. 105835.

TANBAYEV, K. 2022. Working body for intra-soil application of liquid fertilizers. In Materials of the international scientific and practical conference Seifullin readings – 18: "Youth and Science – a Look into the Future". Nur-Sultan, pp. 23–27. ISBN 978-601-257-220-9. (In Russian: Rabochii organ dlya vnutripochvennogo vneseniya zhidkih udobrenii)

TILTON, J. N. 2007. Section 6: Fluid & particle dynamics. In GREEN, D. W. (eds). Perry´s Chemical Engineers´ Handbook, 8th ed. New York, USA : McGraw-Hill Professional, pp. 6–33.

VASILYEV, A. A. – VASILYEV, S. A. – SHKILEV, N. P. 2020. Mechanized spraying of liquid meliorants. In IOP Conference Series: Earth and Environmental Science, vol. 421, no. 3, 032026.

WANG, J. 2011. Theory of flow distribution in manifolds. In Chemical Engineering Journal, vol. 168, no. 3, pp. 1331–1345.

XIUYUN, X. – XUFENG, X. – ZELONG, Z. – BIN, Z. – SHURAN, S. – ZHEN, L. – TIANSHENG, H. – HUIXIAN, H. 2019. Variable rate liquid fertilizer applicator for deep-fertilization in precision farming based on ZigBee technology. In IFAC-PapersOnLine, vol. 52, no. 30, pp. 43–50.

YAMIN, M. – WAN ISMAIL, W. I. – MOHD KASSIM, M. S. – ABD AZIZ, S. – SHAMSHIRI, R. 2016. VRT liquid fertilizer applicator for soil nutrient management. In Jurnal Teknologi, vol. 78, no 1–2, pp. 73–78.